



Effect of Ca addition on microstructure and impression creep behavior of cast AZ61 magnesium alloy

B. NAMI, S. M. MIRE SMAEILI, F. JAMSHIDI, I. KHOUBROU

Department of Materials Engineering and New Technologies,
Shahid Rajaee Teacher Training University, Lavizan, Tehran, Iran

Received 16 September 2018; accepted 8 August 2019

Abstract: Microstructure and creep properties of AZ61 alloy containing 1 and 3 wt.% Ca were investigated. The creep properties were examined using impression method under different stresses between 200 and 500 MPa at the temperature ranging from 423 to 491 K. The microstructure of AZ61 alloy contains $\alpha(\text{Mg})$ matrix and $\text{Mg}_{17}\text{Al}_{12}$ intermetallic phases. It is shown that adding Ca to AZ61 alloy reduces the amount of $\text{Mg}_{17}\text{Al}_{12}$ phase via forming $(\text{Mg},\text{Al})_2\text{Ca}$ phase; furthermore, increasing the Ca content to 3 wt.% leads to the formation of $(\text{Mg},\text{Al})_2\text{Ca}$ phase, as well as the elimination of the $\text{Mg}_{17}\text{Al}_{12}$ phase. Creep properties of AZ61 alloy are improved with the Ca addition. The improvement in creep properties is attributed to the reduction in the amount of $\text{Mg}_{17}\text{Al}_{12}$ phase and the formation of $(\text{Mg},\text{Al})_2\text{Ca}$ phase with high thermal stability. According to the obtained creep data, it is concluded that the pipe diffusion–climb controlled dislocation creep is the dominant creep mechanism and Ca addition has no influence on this mechanism. The effect of pre-deformation on the creep properties of AZ61+3%Ca alloy reveals that the creep resistance of the alloy depends on the continuity of $(\text{Mg},\text{Al})_2\text{Ca}$ phase. It is decreased by reducing the phase continuity.

Key words: impression creep; magnesium alloy; Ca addition; dislocation creep; phase continuity

1 Introduction

Magnesium alloys, as the lightest structural metallic materials, have a great potential for engineering applications, particularly in the electronics, aerospace and automotive industries [1–3]. Among the magnesium alloys, AZ family of these alloys are more attractive because of their good characteristics such as good machinability, acceptable mechanical properties at room temperature, good corrosion resistance and reasonable casting properties [4,5]. AZ61 alloy is one of the common commercial magnesium alloys. The poor mechanical properties, especially creep properties of this alloy at high temperatures, have limited its application at temperatures below 393 K (120 °C) [5]. The presence of $\text{Mg}_{17}\text{Al}_{12}$ intermetallic compound at grain boundaries and interdendritic regions with low melting point leads to low strength and poor creep performance of this alloy at elevated temperatures [6,7]. In many studies, it has been reported that the high-temperature strength of AZ family alloys and similar alloy systems can be improved by adding some alloying elements, such as Si, Ca, Bi, Sr

and rare earth (RE) [8–10]. The improvement in mechanical properties at high temperature by alloying with these elements has been attributed to the formation of thermally-stable intermetallic compounds in the magnesium matrix, reduction in the amount of $\text{Mg}_{17}\text{Al}_{12}$ phase and suppressing the discontinuous precipitation of $\text{Mg}_{17}\text{Al}_{12}$ phase [8–10]. Among the above-mentioned alloying elements, Ca is an effective alloying element for improving mechanical properties of Mg–Al base alloys [11,12]. Effect of adding Ca on microstructure and creep behavior of Mg–Al–Zn alloys has been reported in previous works [13,14]. It has been claimed that the increased creep resistance of the alloys can be attributed to the formation of Al_2Ca intermetallic compound and suppressing formation of $\text{Mg}_{17}\text{Al}_{12}$ phase during the solidification process of the alloy. LI et al [15] have investigated the effect of addition Ca on the microstructure of AZ91D alloy. They have reported that by adding 0.2 and 0.4 wt.% of Ca, no new phase was formed in the microstructure of the alloy and the amount of $\text{Mg}_{17}\text{Al}_{12}$ phase was reduced at the grain boundaries. Also, They suggested that by increasing the quantity of Ca content up to 1 wt.%, the Al_2Ca intermetallic

compounds formed at the grain boundaries with lamellar morphology. KIM et al [16] investigated the effect of Ca contents on hot workability of AZ31 alloy and found that both compression and tensile strength was improved with adding 0.7 and 2 wt.% Ca to the alloy. Improvement in high-temperature mechanical properties of AZ61 alloy has been reported by JUN et al [17]. It has been shown that adding Ca and Y improve the creep properties of the alloy via the formation of Al_2Ca and Al_2Y intermetallic compounds in the microstructure of the alloy. Although some studies have shown that the mechanical properties of Mg–Al–Zn base alloys can be improved by adding certain alloying elements, little is known about the effects of Ca alloying element on the creep behavior of AZ61 alloy. Hence, the aim of the current study is to investigate the creep properties of AZ61 alloy with 1 and 3 wt.% Ca additions in the as-cast condition via impression testing technique. Impression creep test has been developed by CHU and LI [18] and this technique is a modified version of indentation creep test, in which the indenter is a flat-ended cylindrical punch. In this method, the impression depth in a material is recorded versus creep time under constant stress [19–21]. This testing technique has recently been employed for determining creep behavior of different materials, such as magnesium alloys [22–24].

2 Experimental

The alloys were prepared from pure Mg (99.9 wt.%), Al (99.7 wt.%), Zn (99.9 wt.%), Ca (99.8 wt.%) and pure Mn tablets. In this process, magnesium was melted in a graphite crucible using electrical resistance furnace at 750 °C. Argon protective gas and covering flux were used to protect the melt against oxidation and burning. Then, the alloying elements Al, Zn and Mn were added to the melt simultaneously. The mixing operation was performed using a steel rod. After melting the alloying elements, stirring the melt and removing the slag, the melt was poured in a preheated (200 °C) steel mold. In order to prepare the Ca-containing alloys, some part of the AZ61 alloy was re-melted, and then Ca was added to it. Table 1 lists the chemical composition of the prepared alloys used in this research. The samples required for creep test and microstructure investigations were prepared by electro discharge wire-cut machine (with dimensions of 12 mm × 12 mm × 12 mm). Two surfaces of the specimen were prepared using SiC papers with 80, 600, 800 and 1200 grit size before creep testing. The creep test was performed via impression method using a flat-ended cylindrical punch made of tungsten carbide with 2 mm in diameter in the temperature range of 423–491 K under stresses of 200–500 MPa. The penetration depth of the punch was recorded with time

with the accuracy of 1 μm. The microstructural investigations were conducted using scanning electron microscope (SEM). The samples were polished using 0.3 μm alumina powder and distilled water and then etched with acid picric etchant at room temperature.

Table 1 Chemical composition of produced alloys (wt.%)

Alloy	Al	Zn	Mn	Ca	Mg
AZ61	5.58	0.53	0.22	0	Bal.
AZ61+1%Ca	5.70	0.52	0.21	0.85	Bal.
AZ61+3%Ca	5.78	0.60	0.18	2.8	Bal.

3 Results and discussion

3.1 Microstructure before creep

The SEM images of the as-cast AZ61 magnesium alloy are shown in Figs. 1(a) and (b). Considering the binary phase diagram of Mg–Al system [25], it is possible to state that microstructure of the alloy is composed of $\alpha(Mg)$ matrix phase and $\beta(Mg_{17}Al_{12})$ phase distributing in the grain boundaries. SEM image of this alloy in Fig. 1(b) clearly confirms that the intermetallic compounds have two types of massive and lamellar morphologies. The $\beta(Mg_{17}Al_{12})$ phase with massive morphology forms during eutectic reaction in the interdendritic areas. The lamellar $Mg_{17}Al_{12}$ phase forms after solidification and during the alloy cooling process due to the decreased aluminum solubility. Supersaturated phase with dark contrast is seen around the intermetallic phases and interdendritic areas shown in Fig. 1(a) (Point B). The intermetallic phases are mostly surrounded by supersaturated magnesium phase containing aluminum content higher than that of other areas in the $\alpha(Mg)$ matrix phase, as revealed by EDS analysis given in Table 2. Similar microstructural features have been reported for the as-cast AZ61 alloy [5,26]. The SEM images of the as-cast AZ61+1%Ca magnesium alloy are shown in Figs. 1(c) and (d). The images confirm that three phases form in the microstructure of the alloy. The EDS analysis of the different phases is given in Table 2. As can be estimated from Table 2, the areas corresponding to the Points B and C may be $Mg_{17}Al_{12}$ intermetallic compounds with two types of massive and lamellar morphologies, respectively. The solubility of Ca in the $\alpha(Mg)$ matrix is negligible and it is segregated at the grain boundaries. Chemical composition of the Ca-containing phase in Table 2 also indicates that it must be $(Mg,Al)_2Ca$ intermetallic compound. Although Al_2Ca is the stable compound in the microstructure of Mg–Al–Ca alloys solidified under equilibrium condition [27], $(Mg,Al)_2Ca$ phase with C36 structure is observed in the microstructure of those alloys cooled under non-equilibrium conditions [28]. The SEM images of the

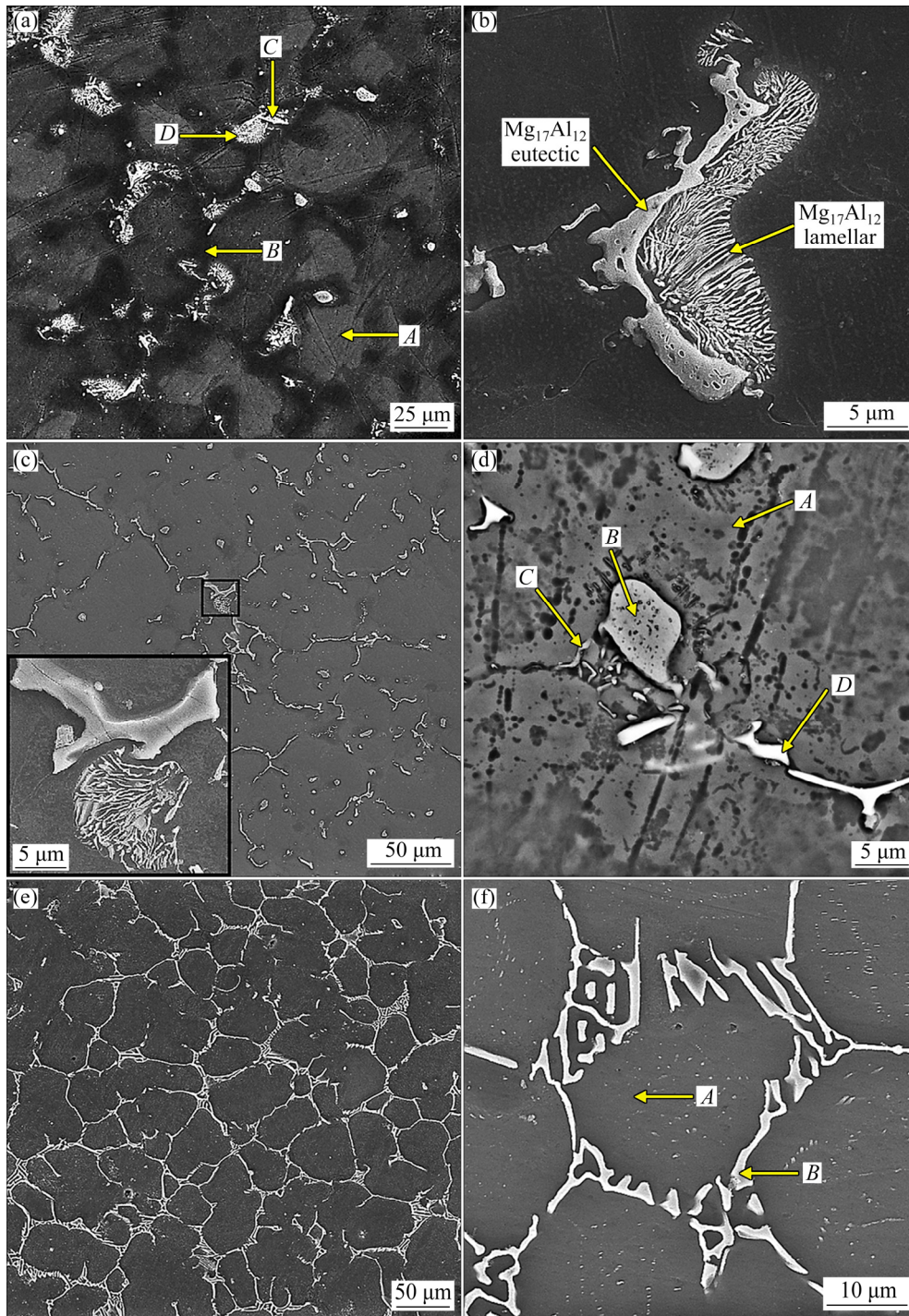


Fig. 1 SEM images of alloys with different magnifications: (a, b) AZ61; (c, d) AZ61+1%Ca; (e, f) AZ61+3%Ca

as-cast AZ61+3%Ca magnesium alloy are shown in Figs. 1(e) and (f). As seen, the microstructure of the alloy consists of the matrix phase and intermetallic compounds.

According to the EDS results given in Table 2, the intermetallic compound in the microstructure of the alloy is $(\text{Mg,Al})_2\text{Ca}$. Comparing the microstructure of 3% Ca-containing AZ61 alloy with 1% Ca alloy reveals that increasing the Ca content to 3% leads to the removal of

the $\text{Mg}_{17}\text{Al}_{12}$ phase, as well as, the formation of the coarse $(\text{Mg,Al})_2\text{Ca}$ compounds with continuous network structure in the microstructure. Comparing Fig. 1(a) with Fig. 1(e) indicates that the refinement of dendrite size and morphology is the other effect of Ca addition on the microstructure of AZ61 alloy. The EDS results show that Ca element has no solubility in the $\alpha(\text{Mg})$ matrix and this element mainly segregates on the grain boundary. Therefore, it is expected that a larger volume fraction of

Table 2 EDS results of selected points of alloys (wt.%)

Alloy	Point	Al	Zn	Mn	Ca	Mg
AZ61	A	2.43	0.61	0.16	0	Bal.
	B	8.34	0.46	0	0	Bal.
	C	24.43	0.24	0	0	Bal.
	D	15.21	0.15	0	0	Bal.
AZ61+1%Ca	A	2.69	0.49	0.12	0.07	Bal.
	B	37.68	0	0	0.14	Bal.
	C	17.31	0	0	0.04	Bal.
	D	52.75	0	0	22.89	Bal.
AZ61+3%Ca	A	0.97	0.72	0.33	0	Bal.
	B	31.99	0	0	13.22	Bal.

(Mg,Al)₂Ca phase forms at the grain boundaries with increasing Ca content, as shown in Fig. 1(e). Formation of (Mg,Al)₂Ca phase consumes the Al content, resulting in decreasing Mg₁₇Al₁₂ phase content.

3.2 Creep properties

Figure 2 typically shows the impression depth curves and variations of impression rate with creep time for AZ61, AZ61+1%Ca and AZ61+3% alloys tested at 476 K under different stresses. It can be seen that the creep curves are composed of two regions. In the first region of creep, called primary creep, the impression rate is reduces with time. In the second region of creep, the impression depth linearly increases with time, and the impression rate remains constant, which is called

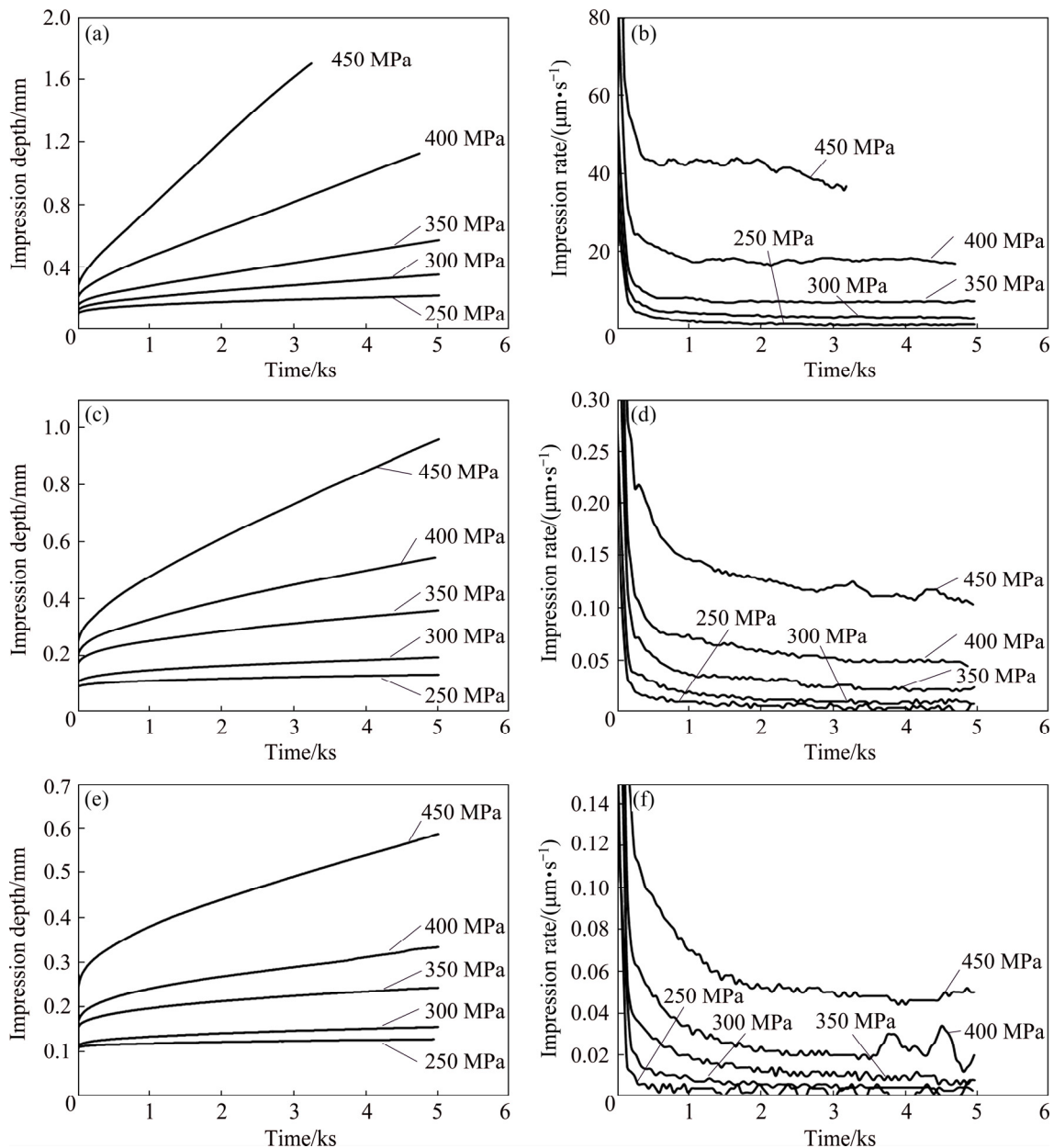


Fig. 2 Curves of impression depth (a, c, e) and impression rate (b, d, f) variations with creep time at 476 K: (a, b) AZ61; (c, d) AZ61+1%Ca; (e, f) AZ61+3%Ca

secondary creep or steady state. Tertiary creep is not observed on these curves due to the compressive nature of the used stress during impression creep tests. According to this figure, it is perceived that the slope of the curves in the steady state creep region raises by increasing the applied stress. So, at a specific creep time, the impression depth increases by increasing either applied stress or temperature.

Figure 3 shows the curves of impression depth and variations of impression rate with creep time for all three alloys at 447 K and stress of 450 MPa. It can be observed that the Ca addition causes a significant increase in creep resistance of AZ61 alloy. This effect is more pronounced for AZ61+3%Ca alloy, which may be attributed to the microstructural variations resulted from the Ca addition to the alloy.

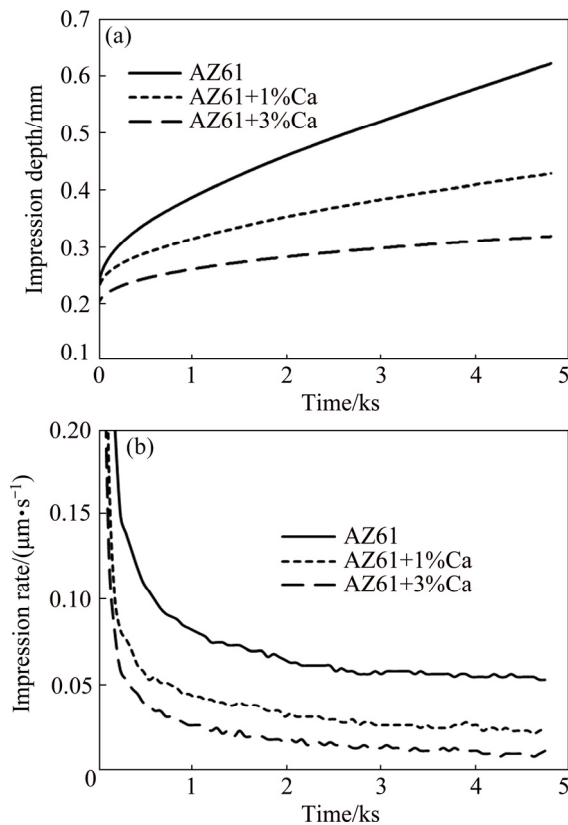


Fig. 3 Curves of impression creep at 447 K and 450 MPa: (a) Variation of impression depth with creep time; (b) Variation of impression rate with creep time

3.3 Creep mechanisms

Creep mechanism could be determined either by microstructure investigation using transmission electron microscope (TEM) or calculating the stress exponent and activation energy of creep based on the power law equation [24]. For the impression creep test, the relationship between the impression velocity, V_{imp} , and the punching stress, σ_{imp} , is obtained in the following equation [29–31]:

$$\left(\frac{V_{\text{imp}}T}{G}\right) = A \left(\frac{\varphi C_2}{C_1^n}\right) \left(\frac{b}{d}\right)^p \left(\frac{bD_0}{K}\right) \left(\frac{\sigma_{\text{imp}}}{G}\right)^n \exp\left(\frac{-Q_c}{RT}\right) \quad (1)$$

where A , C_1 and C_2 are dimensionless constants, φ is the diameter of the punch, b is the absolute value of Burgers vector, d is the grain size, p is the grain size power, D_0 is the appropriate diffusion coefficient constant, G is the shear modulus, K is the Boltzmann's constant, T is the test temperature, n is the stress exponent, Q_c is the creep activation energy and R is the universal gases constant. According to Eq. (1), stress exponent, n , and activation energy, Q_c , can be determined from the slope of the best-fit line to the variations of $\ln(V_{\text{imp}}T/G)$ with $\ln(\sigma_{\text{imp}}/G)$ at constant temperature and $\ln(V_{\text{imp}}T/G)$ with $1/T$ at constant values of σ_{imp}/G , respectively. The shear modulus of AZ61 magnesium alloy is calculated from the following equation [32]:

$$G/\text{MPa} = 15400 - 18(T/\text{K} - 400) \quad (2)$$

Figure 4 shows the variations of $\ln(V_{\text{imp}}T/G)$ with $\ln(\sigma_{\text{imp}}/G)$ for all alloys at the temperatures between 423 and 491 K. As can be seen, variations of $\ln(V_{\text{imp}}T/G)$ with $\ln(\sigma_{\text{imp}}/G)$ are linear and the stress exponents or the slope of the lines varies between 4.14 and 6.6 for all alloys. Comparison of the results indicates that Ca has no effect on the stress exponents and the stress exponent increases by increasing temperature for all alloys. As previously said, the creep mechanism can be estimated by calculating the stress exponent. According to the literatures [33,34], the stress exponent between 4 and 6 is related to the climb-controlled dislocation creep in which the creep rate is controlled by edge dislocation climbing. So, it can be said that the climb-controlled dislocation creep is the dominant creep mechanism under the test conditions used in the current study. Figure 5 shows the variations of $\ln(V_{\text{imp}}T/G)$ with the reciprocal of temperature under constant normalized stresses for all alloys. The apparent activation energies for creep are determined from the slope of lines. It is observed that values of the activation energy are between activation energy of pipe diffusion (92 kJ/mol) and lattice diffusion (135 kJ/mol) of magnesium for AZ61 alloy. As seen in Figs. 5(b) and (c), the creep activation energy is decreased by increasing the Ca content and its values are slightly less than those for magnesium pipe diffusion. The creep activation energy between that for lattice and pipe diffusion of magnesium atoms is carried out simultaneously and in parallel during creep process [13]. In such a situation, it has been stated that one of the mechanisms is dominant, which can be specified by comparing the obtained creep activation energy with the critical activation energy of about 113 kJ/mol reported in the previous investigations [33]. Lattice diffusion is the

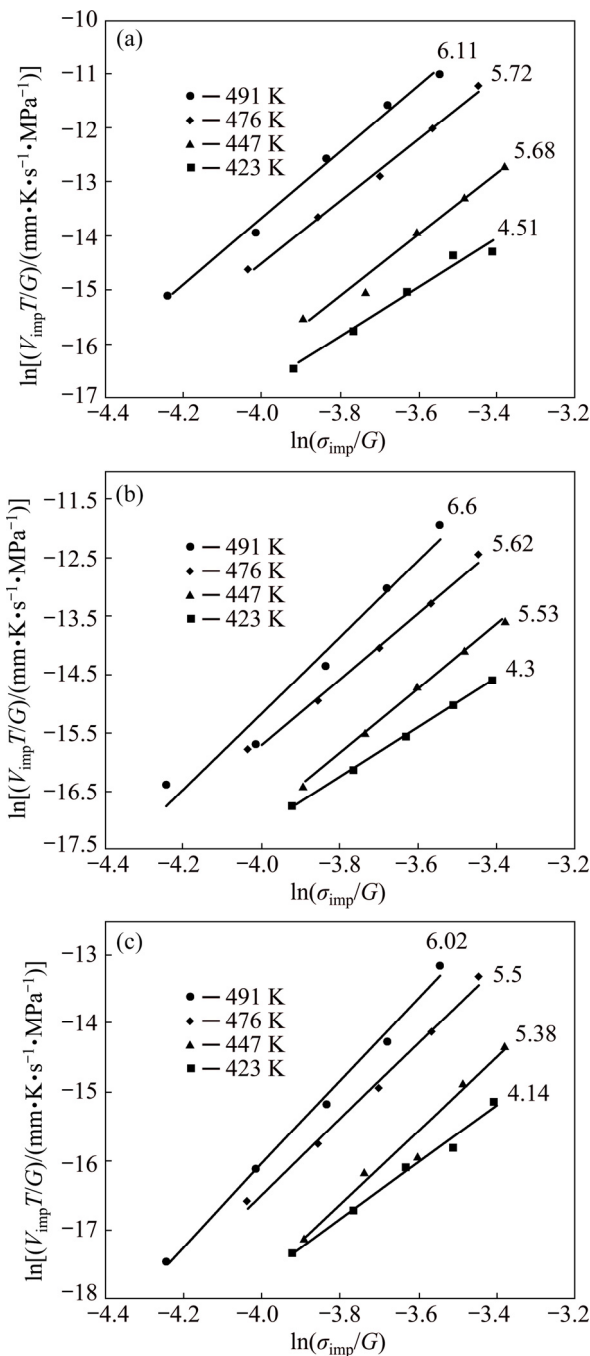


Fig. 4 Normalized minimum impression velocity as function of normalized punching stress at different temperatures: (a) AZ61; (b) AZ61+1%Ca; (c) AZ61+3%Ca

dominant mechanism for the creep process with the activation energies more than the critical activation energy. Pipe diffusion of magnesium atoms is the dominant mechanism if the creep activation energy is less than the critical energy. Considering this hypothesis and the obtained results in Fig. 5 reveals that magnesium diffusion in dislocation pipe is dominant during the tests. The dislocation creep in which the creep rate is controlled by climbing dislocation and the atoms diffusion is carried out in dislocation pipe is known as

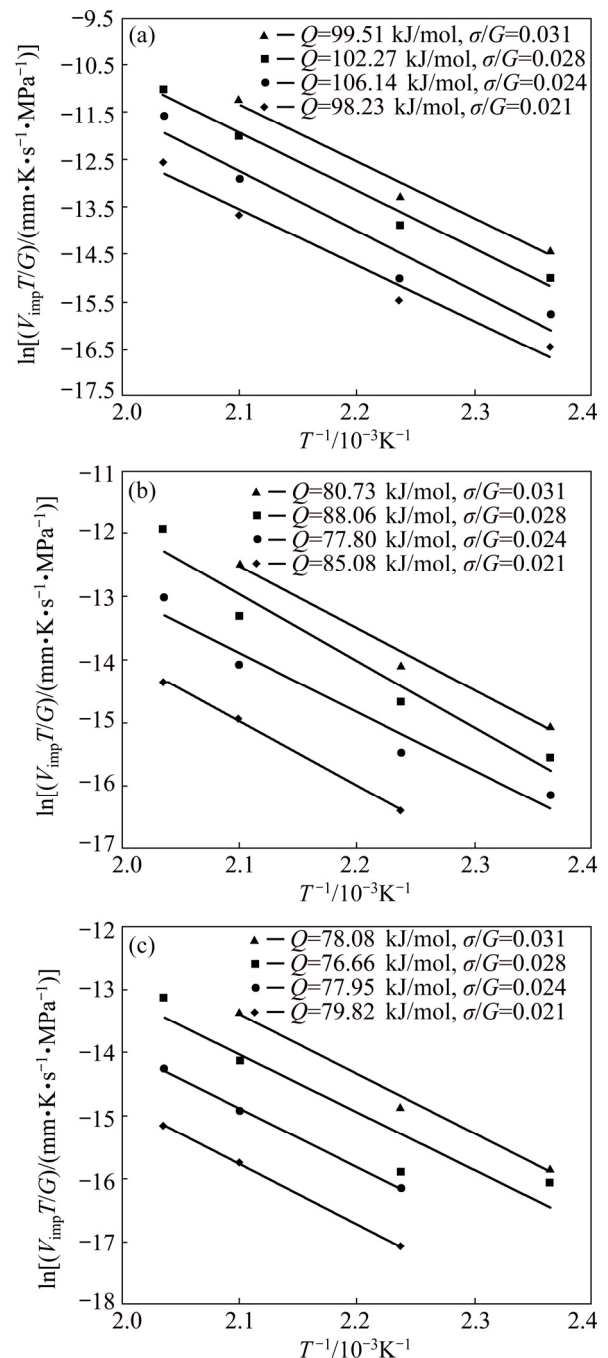


Fig. 5 Temperature dependence of normalized minimum impression velocity at different constant normalized punching: (a) AZ61; (b) AZ61+1%Ca; (c) AZ61+3%Ca

pipe diffusion-climb controlled dislocation creep [32]. As shown in Figs. 4 and 5, Ca addition has no considerable influence on the stress exponents and activation energies. The similar values of the stress exponents and creep activation energies of the alloys reveal that Ca has no effect on the dominant creep mechanism. In this deformation mechanism, large intermetallic particles having high thermal stability on the grain boundaries, reduction in the amount of $Mg_{17}Al_{12}$ phase and lowering stacking fault energy (SFE)

can improve the creep properties of the Mg–Al based alloys [29]. The improvement in creep resistance of AZ61+1%Ca alloy can be also attributed to the presence of $(\text{Mg,Al})_2\text{Ca}$ intermetallic phase with high thermal stability in the interdendritic regions and reduction in the amount of $\text{Mg}_{17}\text{Al}_{12}$ phase. Comparing the creep properties of the alloys in Fig. 3 indicates that much improvement in creep properties is obtained with increasing the Ca content to 3 wt.%. This can be attributed to the complete removal of $\text{Mg}_{17}\text{Al}_{12}$ phase and the formation of $(\text{Mg,Al})_2\text{Ca}$ intermetallic phase with continuous network in the microstructure of the alloy. The presence of grain boundary sliding in the dislocation creep has been previously reported in Ref. [13]. Therefore, the formation of continuous intermetallic compound with high thermal stability in AZ61+3%Ca alloy will improve the creep properties, as shown in Fig. 3, by reducing grain boundary sliding. Comparing the chemical composition of AZ61 and AZ61+3%Ca alloys indicates that the solubility of aluminum in the matrix phase is decreased from 2.43 to 0.97. It has been reported that SFE of magnesium is reduced by increasing aluminum content [32]. So, it is revealed that Ca addition reduces the creep properties of matrix phase via decreasing SFE.

In order to investigate the effect of continuity of the $(\text{Mg,Al})_2\text{Ca}$ intermetallic compounds on creep resistance of AZ61+3%Ca alloy, the alloy was compressed at ambient temperature. The deformation rate is calculated from the following equation:

$$R=(d_0-d)/d_0 \quad (3)$$

where d_0 and d are the thickness of the sample before and after the deformation, respectively.

Figure 6 shows the creep behavior of the deformed and non-deformed cast samples of AZ61+3%Ca alloy at 476 K and stress of 350 MPa. As can be seen, applying a deformation rate of 10% on this alloy leads to an increase in the steady state rate and reduction in the creep resistance. In addition, by increasing the deformation rate to 20%, there is more increase in the steady state creep rate. The presence of micro crack inside $(\text{Mg,Al})_2\text{Ca}$ phase is seen in Fig. 7 which reduces the phase continuity. This indicates that in addition to thermal stability of the $(\text{Mg,Al})_2\text{Ca}$ phase, the continuity of $(\text{Mg,Al})_2\text{Ca}$ intermetallic compounds is responsible for the increased creep resistance of these alloys.

3.4 Constitutive equations

The constitutive equation, describing the material deformation behavior under different conditions, is generally expressed as Eq. (1) by assuming $C_1=3$, $C_2=1$. The creep strain rate, $\dot{\epsilon}$, and stress, σ , in tensile creep equal $V_{\text{imp}}/C_2\varphi$ and σ_{imp}/C_1 , respectively [29–31,35]. The

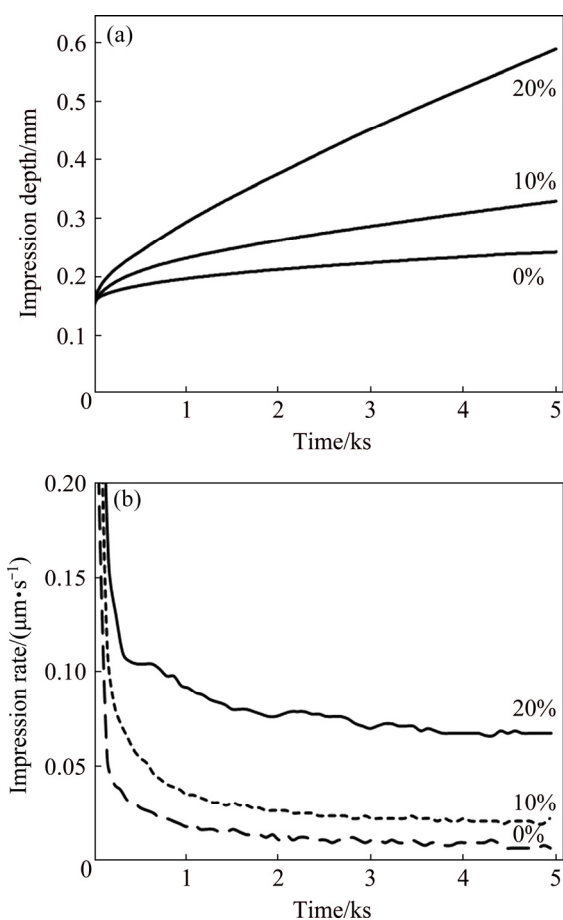


Fig. 6 Impression creep curves of deformed and non-deformed cast samples of AZ61+3%Ca alloy at 476 K and 350 MPa: (a) Variation of impression depth with creep time; (b) Variation of impression rate with creep time

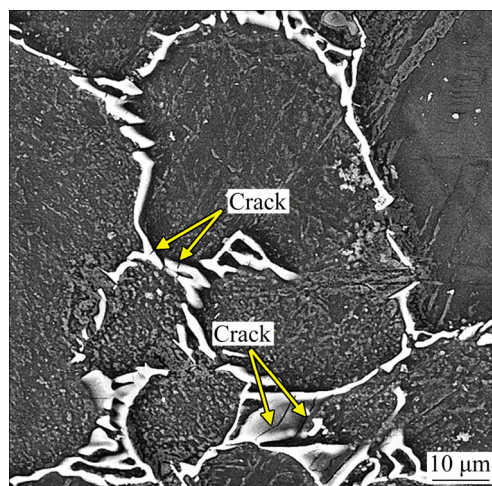


Fig. 7 SEM image of AZ61+3%Ca alloy after 10% deformation

creep strain rate is normalized and the relationship between $(\dot{\epsilon}/D)[kT/(Gb)]$ and (σ/G) is shown in Fig. 8. The diffusion coefficients, D , for AZ61, AZ61+1%Ca, and AZ61+3%Ca alloys are taken to be that for pipe diffusion coefficient in pure magnesium. It can be

observed that, the data for each of the alloys are aligned along a straight line with a slope of 5.1, 6 and 5.8 for AZ61, AZ61+1%Ca and AZ61+3%Ca alloys, respectively. As seen, the addition of Ca to AZ61 alloy has no distinct influence on the stress exponents and the creep rate is decreased by adding Ca element at different stresses and temperatures.

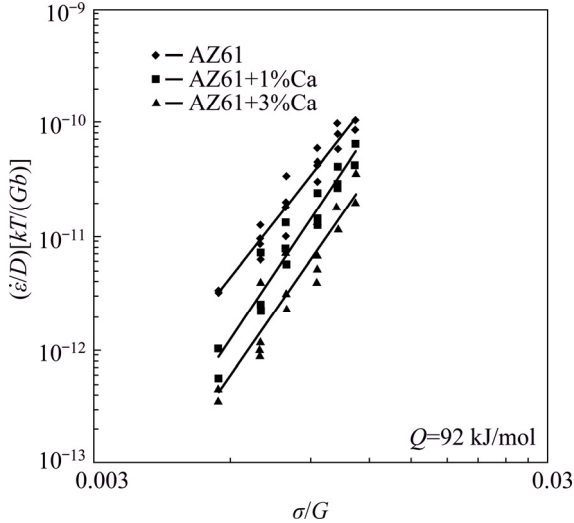


Fig. 8 Relationship between $(\dot{\epsilon}/D)[kT/(Gb)]$ and (σ/G) for alloys

The constitutive equations for the present alloys are obtained by the best fit of the data points in Fig. 8:

$$\dot{\epsilon}_{AZ61} = 0.93[Gb/(kT)]/[(\sigma/G)^{5.1}D] \quad (4)$$

$$\dot{\epsilon}_{AZ61+1\%Ca} = 32.14[Gb/(kT)]/[(\sigma/G)^{6.0}D] \quad (5)$$

$$\dot{\epsilon}_{AZ61+3\%Ca} = 5.17[Gb/(kT)]/[(\sigma/G)^{5.8}D] \quad (6)$$

The stress exponents and pre-exponential constants are determined from the slope and the intercept of the lines, respectively.

3.5 Microstructure after creep

Figure 9 shows the microstructure after creep testing at 476 K and stress of 350 MPa around the indented edges for AZ61 and AZ61+3%Ca alloys. Three distinct areas are seen in the microstructure of the alloys after impression creep test. In Area 1, located exactly under the punch, no deformation is seen. Results of the previous investigation indicate that the stress distribution in this region is hydrostatic. So, the plastic deformation does not take place in this area. Similarly, considerable deformation is not seen in the region far from the indenter in Area 3. Flowing of materials is clearly seen in Area 2. The intermetallic compound has been aligned and strained along the flow direction of the materials. Comparing microstructure of the crept AZ61 and AZ61+3%Ca alloys reveals that the Area 2 or plastic deformation region in AZ61+3%Ca alloy is smaller than

that in AZ61 alloy, which can be attributed to the presence of continuous $(Mg,Al)_2Ca$ phase with high thermal stability in the interdendritic regions.

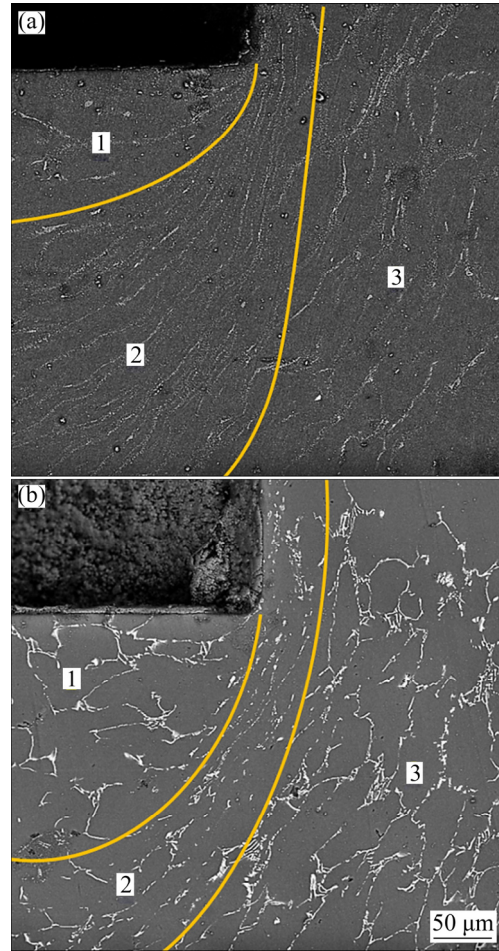


Fig. 9 Cross-sectional morphologies of impression edge after creep test at 476 K and 350 MPa: (a) AZ61; (b) AZ61+3%Ca

4 Conclusions

(1) The microstructure of AZ61 alloy in the as-cast condition contains $\alpha(Mg)$ matrix and $Mg_{17}Al_{12}$ intermetallic phases. Adding 1 wt.% Ca to AZ61 alloy results in the reduction of the amount of $Mg_{17}Al_{12}$ phase and the formation of $(Mg,Al)_2Ca$ intermetallic compounds in the interdendritic regions. By increasing the amount of Ca to 3 wt.%, the $Mg_{17}Al_{12}$ phase is removed and $(Mg,Al)_2Ca$ intermetallic phase with continuous network forms in the microstructure of AZ61+3%Ca alloy.

(2) Creep properties of AZ61 alloy are improved due to Ca addition. The improvement of creep properties is attributed to the reduction in the amount of thermally-unstable $Mg_{17}Al_{12}$ phase and the formation of $(Mg,Al)_2Ca$ phase with high thermal stability for AZ61+1%Ca alloy and the removal of $Mg_{17}Al_{12}$ phase and the formation of continuous $(Mg,Al)_2Ca$ phase for

AZ61+3%Ca alloy.

(3) Calculating values of stress exponent and activation energy under the experimental condition reveal that dislocation climb controlled by pipe diffusion is the dominant mechanism during the creep of AZ61, AZ61+1%Ca and AZ61+3%Ca alloys and Ca has no influence on the creep mechanism.

(4) Applying the compressive deformation reduces creep strength of the AZ61+3%Ca alloy, which can be attributed to the reduction of the continuity of (Mg,Al)₂Ca intermetallic phase.

References

- [1] SURESH K, RAO K P, PRASAD Y V R K, HORT N, DIERINGA H. Hot forging of Mg–4Al–2Ba–2Ca (ABaX422) alloy and validation of processing map [J]. *Transactions of Nonferrous Metals Society of China*, 2018, 28: 1495–1503.
- [2] YU D, ZHANG D, SUN J, LUO Y, XU J, ZHANG H, PAN F. Improving mechanical properties of ZM61 magnesium alloy by aging before extrusion [J]. *Journal of Alloys and Compounds*, 2017, 690: 553–560.
- [3] WU Y P, XIONG H Q, JIA Y Z, XIE S H, LI G F. Microstructure, texture and mechanical properties of Mg–8Gd–4Y–1Nd–0.5 Zr alloy prepared by pre-deformation annealing, hot compression and ageing [J]. *Transactions of Nonferrous Metals Society of China*, 2019, 29: 976–983.
- [4] DING Z B, ZHAO Y H, LU R P, YUAN M N, WANG Z J, LI H J, HUA H O U. Effect of Zn addition on microstructure and mechanical properties of cast Mg–Gd–Y–Zr alloys [J]. *Transactions of Nonferrous Metals Society of China*, 2019, 29: 722–734.
- [5] MAZRAESHAHI E M, NAMI B, MIRE SMAEILI S M. Investigation on the impression creep properties of a cast Mg–6Al–1Zn magnesium alloy [J]. *Materials and Design*, 2013, 51: 427–431.
- [6] SRINIVASAN A, AJITHKUMAR K K, SWAMINATHAN J, PILLAI U T S, PAI B C. Creep behavior of AZ91 magnesium alloy [J]. *Procedia Engineering*, 2013, 55: 109–113.
- [7] MAZRAESHAHI E M, NAMI B, MIRE SMAEILI S M, TABATABAEI S M. Effect of Si on the creep properties of AZ61 cast magnesium alloy [J]. *Materials and Design*, 2015, 76: 64–70.
- [8] ZHANG Y, YANG L, DAI J, GUO G, LIU Z. Effect of Ca and Sr on microstructure and compressive creep property of Mg–4Al–RE alloys [J]. *Materials Science and Engineering A*, 2014, 610: 309–314.
- [9] ZHANG D, ZHANG D, BU F, LI X, GUAN K, YANG Q, LIU S, LIU X, MENG J. Effects of minor Sr addition on the microstructure, mechanical properties and creep behavior of high pressure die casting AZ91–0.5RE based alloy [J]. *Materials Science and Engineering A*, 2017, 693: 51–59.
- [10] JING B, YANGSHAN S, SHAN X, FENG X, TIANBAI Z. Microstructure and tensile creep behavior of Mg–4Al based magnesium alloys with alkaline-earth elements Sr and Ca additions [J]. *Materials Science and Engineering A*, 2006, 419: 181–188.
- [11] DU Y Z, QIAO X G, ZHENG M Y, WANG D B, WU K, GOLOVIN I S. Effect of microalloying with Ca on the microstructure and mechanical properties of Mg–6mass%Zn alloys [J]. *Materials and Design*, 2016, 98: 285–293.
- [12] KONDARI B, MAHMUDI R. Effect of Ca additions on the microstructure and creep properties of a cast Mg–Al–Mn magnesium alloy [J]. *Materials Science and Engineering A*, 2017, 700: 438–447.
- [13] NAMI B, RAZAVI H, MIRDAMADI S, SHABESTARI S G, MIRE SMAEILI S M. Effect of Ca and rare earth elements on impression creep properties of AZ91 magnesium alloy [J]. *Metallurgical and Materials Transactions A*, 2010, 41: 1973–1982.
- [14] NAMI B, SHABESTARI S G, RAZAVI H, MIRDAMADI S, MIRE SMAEILI S M. Effect of Ca, RE elements and semi-solid processing on the microstructure and creep properties of AZ91 alloy [J]. *Materials Science and Engineering A*, 2011, 528: 1261–1267.
- [15] LI S S, TANG B, ZENG D B. Effects and mechanism of Ca on refinement of AZ91D alloy [J]. *Journal of Alloys and Compounds*, 2007, 437: 317–321.
- [16] KIM J H, KANG N E, YIM C D, KIM B K. Effect of Ca content on the microstructural evolution and mechanical properties of wrought Mg–3Al–1Zn alloy [J]. *Materials Science and Engineering A*, 2009, 525: 18–29.
- [17] CHEN Jun, ZHANG Qing, LI Quan-an. Effect of Y and Ca addition on the creep behaviors of AZ61 magnesium alloys [J]. *Journal of Alloys and Compounds*, 2016, 686: 375–383.
- [18] CHU S N G, LI J C M. Impression creep: A new creep test [J]. *Journal of Materials Science*, 1977, 12: 2200–2208.
- [19] SASTRY D H. Impression creep technique—An overview [J]. *Materials Science and Engineering A*, 2005, 409: 67–75.
- [20] LI J C. Impression creep and other localized tests [J]. *Materials Science and Engineering A*, 2002, 322: 23–42.
- [21] YANG F, LI J C. Impression test—A review [J]. *Materials Science and Engineering R*, 2013, 74: 233–253.
- [22] GANGULY S, MONDAL A K. Influence of SiC nanoparticles addition on microstructure and creep behavior of squeeze-cast AZ91–Ca–Sb magnesium alloy [J]. *Materials Science and Engineering A*, 2018, 718: 377–389.
- [23] WANG H, WANG Q D, BOEHLERT C J, YANG J, YIN D D, YUAN J, DING W J. The impression creep behavior and microstructure evolution of cast and cast-then-extruded Mg–10Gd–3Y–0.5 Zr (wt.%) [J]. *Materials Science and Engineering A*, 2016, 649: 313–324.
- [24] KHALILPUOR H, MIRE SMAEILI S M, BAGHANI A. The microstructure and impression creep behavior of cast Mg–4Sn–4Ca alloy [J]. *Materials Science and Engineering A*, 2016, 652: 365–369.
- [25] DAHLE A K, LEE Y C, NAVE M D, SCHAFFER P L, STJOHN D H. Development of the as-cast microstructure in magnesium–aluminum alloys [J]. *Journal of Light Metals*, 2001: 61–72.
- [26] YAN X U, HU L X, YU S U N, JIA J B, JIANG J F. Microstructure and mechanical properties of AZ61 magnesium alloy prepared by repetitive upsetting-extrusion [J]. *Transactions of Nonferrous Metals Society of China*, 2015, 25: 381–388.
- [27] OZTURK K, ZHONG Y, LIU Z K, LUO A A. Creep resistant Mg–Al–Ca alloys: Computational thermodynamics and experimental investigation [J]. *Journal of the Minerals, Metals & Materials Society (TMS)*, 2003, 55: 40–44.
- [28] SUZUKI A, SADOCK N D, JONES J W, POLLOCK T M. Solidification paths and eutectic intermetallic phases in Mg–Al–Ca ternary alloys [J]. *Acta Materialia*, 2005, 53: 2823–2834.
- [29] NAMI B, RAZAVI H, MIRE SMAEILI S M, MIRDAMADI S, SHABESTARI S G. Impression creep properties of a semi-solid processed magnesium–aluminum alloy containing Ca and rare earth elements [J]. *Scripta Materialia*, 2011, 65: 221–224.
- [30] ESGANDARI B A, NAMI B, SHAHMIRI M, ABEDI A. Effect of Mg and semi solid processing on microstructure and impression creep properties of A356 alloy [J]. *Transactions of Nonferrous Metals Society of China*, 2013, 23: 2518–2523.
- [31] MIRE SMAEILI S M, NAMI B, ABBASI R, KHOUBROU I. Effect of Cu on the creep behavior of cast Al–15Si–0.5Mg alloy [J]. *Journal of the Minerals, Metals & Materials Society (TMS)*, 2019, 71: 2128–2135.

- [32] SOMEKAWA H, HIRAI K, WATANABE H, TAKIGAWA Y, HIGASHI K. Dislocation creep behavior in Mg–Al–Zn alloys [J]. *Materials Science and Engineering A*, 2005, 407: 53–61.
- [33] KABIRIAN F, MAHMUDI R. Impression creep behavior of a cast AZ91 magnesium alloy [J]. *Metallurgical and Materials Transactions A*, 2009, 40: 116–127.
- [34] RASHNO S, NAMI B, MIRE SMAEILI S M. Impression creep behavior of a cast MRI153 magnesium alloy [J]. *Materials and Design*, 2014, 60: 289–294.
- [35] KHOUBROU I, NAMI B, MIRE SMAEILI S M. Investigation on the creep behavior of AZ91 magnesium alloy processed by severe plastic deformation [J]. *Metals and Materials International*, 2019, Published online.

Ca 对铸态 AZ61 镁合金显微组织和压入蠕变行为的影响

B. NAMI, S. M. MIRE SMAEILI, F. JAMSHIDI, I. KHOUBROU

Department of Materials Engineering and New Technologies,
Shahid Rajaei Teacher Training University, Lavizan, Tehran, Iran

摘要: 研究含 1%和 3%(质量分数)Ca 的 AZ61 镁合金的显微组织和蠕变性能。用压痕法研究在 423~491 K、200~500 MPa 应力作用下的蠕变性能。AZ61 合金的显微组织包含 $\alpha(\text{Mg})$ 基体相和 $\text{Mg}_{17}\text{Al}_{12}$ 金属间化合物相。结果表明, 在 AZ61 合金中加入 Ca 可通过形成 $(\text{Mg},\text{Al})_2\text{Ca}$ 相从而减少 $\text{Mg}_{17}\text{Al}_{12}$ 相含量, 当 Ca 含量达到 3%时, 形成 $(\text{Mg},\text{Al})_2\text{Ca}$ 相, $\text{Mg}_{17}\text{Al}_{12}$ 相消失。Ca 的加入可以改善 AZ61 合金的蠕变性能, 这是由于 $\text{Mg}_{17}\text{Al}_{12}$ 相减少而形成的 $(\text{Mg},\text{Al})_2\text{Ca}$ 相具有高的热稳定性。根据蠕变数据可以推断, 管扩散-攀移控制的位错蠕变是主要的蠕变机制, Ca 添加对此机制没有影响。预变形对 AZ61+3%Ca 合金蠕变性能的影响表明, 合金的抗蠕变性能取决于 $(\text{Mg},\text{Al})_2\text{Ca}$ 相的连续性, 该相的连续性越低, 合金的抗蠕变性能就越差。

关键词: 压入蠕变; 镁合金; Ca 添加; 位错蠕变; 相连续性

(Edited by Bing YANG)